Cellular Signalling 109 (2023) 110805

Contents lists available at ScienceDirect

Cellular Signalling

journal homepage: www.elsevier.com/locate/cellsig

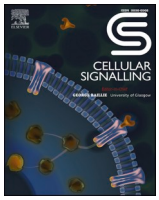

Indicator-dependent differences in detection of local intracellular Ca^{2+} release events evoked by voltage-gated Ca^{2+} entry in pancreatic β-cells

Mingyu Yang, Oleg Dyachok, Yunjian Xu, Erik Gylfe, Olof Idevall-Hagren, Anders Tengholm *

Department of Medical Cell Biology, Uppsala University, Biomedical Centre, Box 571, SE-75123 Uppsala, Sweden

ARTICLE INFO

Keywords:
Ca^{2+} oscillations
R-GECO1
Fluo-5F
Fluo-4
$P2Y_1$ receptor
Insulin secretion
TIRF microscopy

ABSTRACT

Genetically encoded Ca^{2+} indicators have become widely used in cell signalling studies as they offer advantages over cell-loaded dye indicators in enabling specific cellular or subcellular targeting. Comparing responses from dye and protein-based indicators may provide information about indicator properties and cell physiology, but side-by-side recordings in cells are scarce. In this study, we compared cytoplasmic Ca^{2+} concentration ($[Ca^{2+}]_i$) changes in insulin-secreting β-cells recorded with commonly used dyes and indicators based on circularly permuted fluorescent proteins. Total internal reflection fluorescence (TIRF) imaging of K^+ depolarization-triggered submembrane $[Ca^{2+}]_i$ increases showed that the dyes Fluo-4 and Fluo-5F mainly reported stable $[Ca^{2+}]_i$ elevations, whereas the proteins R-GECO1 and GCaMP5G more often reported distinct $[Ca^{2+}]_i$ spikes from an elevated level. $[Ca^{2+}]_i$ spiking occurred also in glucose-stimulated cells. The spikes reflected Ca^{2+} release from the endoplasmic reticulum, triggered by autocrine activation of purinergic receptors after exocytotic release of ATP and/or ADP, and the spikes were consequently prevented by SERCA inhibition or $P2Y_1$-receptor antagonism. Widefield imaging, which monitors the entire cytoplasm, increased the spike detection by the Ca^{2+} dyes. The indicator-dependent response patterns were unrelated to Ca^{2+} binding affinity, buffering and mobility, and probably reflects the much slower dissociation kinetics of protein compared to dye indicators. Ca^{2+} dyes thus report signalling within the submembrane space excited by TIRF illumination, whereas the protein indicators also catch Ca^{2+} events originating outside this volume. The study highlights that voltage-dependent Ca^{2+} entry in β-cells is tightly linked to local intracellular Ca^{2+} release mediated *via* an autocrine route that may be more important than previously reported direct Ca^{2+} effects on phospholipase C or on intracellular channels mediating calcium-induced calcium release.

1. Introduction

The knowledge about Ca^{2+} signalling kinetics in many types of cells largely relies on studies using fluorescent indicators based on Ca^{2+} chelator-conjugated dyes. A prime example is Fura-2, which exhibits a Ca^{2+}-dependent shift in excitation spectrum, allowing ratiometric recordings of the cytoplasmic Ca^{2+} concentration ($[Ca^{2+}]_i$) [1]. Fura-2 requires dual wavelength ultraviolet excitation, which limits its utility in many applications, but there is a number of visible-wavelength intensiometric indicators with different spectral properties and Ca^{2+}-binding affinities, including *e.g.* Fluo-4 [2], Fluo-5F [3], Fura Red [4] and Cal-590 [5]. The fluorescent dyes are convenient to use and can be loaded into most types of cells as membrane permeant acetoxymethyl esters, but they may also negatively influence cell behaviour by Ca^{2+} buffering [6] or other means [7].

The advent of fluorescent proteins enabled development of genetically encoded Ca^{2+} indicators. Many of these sensors are based on calmodulin and the Ca^{2+}/calmodulin binding peptide M13 from myosin light chain kinase [8–10]. Binding of Ca^{2+} induces a conformational change, which can be read out by Förster resonance energy transfer between matching pairs of fluorescent proteins [8] or as a change in intensity of a circularly permuted (cp) fluorescent protein, such as G-CaMP and G-GECO, based on cpGFP [9,10], and R-GECO1, based on red fluorescent cp-mApple [10]. As they require transfection or transduction for expression, genetically encoded Ca^{2+} indicators are unsuitable for some applications but, on the other hand, provide advantages in allowing transgenic expression in experimental animals and/or targeting to specific cell populations or subcellular localizations. Although genetically encoded indicators have been well characterized and proven useful to record $[Ca^{2+}]_i$ signals in a variety of applications both *in vitro*

* Corresponding author.
E-mail address: Anders.Tengholm@mcb.uu.se (A. Tengholm).

https://doi.org/10.1016/j.cellsig.2023.110805
Received 18 May 2023; Received in revised form 22 June 2023; Accepted 8 July 2023
Available online 10 July 2023

and *in vivo*, few studies have made direct comparisons with fluorescent dyes in physiologically relevant systems [6,11].

In pancreatic β-cells, Ca^{2+} signalling has been extensively studied with dye indicators for more than thirty years [12–14]. Glucose is the main physiological stimulus, which at concentrations above 5–7 mM induces $[Ca^{2+}]_i$ elevation, often manifested as oscillations with both slow (0.2–0.5 min^{-1}) and fast (2–5 min^{-1}) patterns [15]. The underlying mechanism is an increase of the ATP/ADP ratio caused by glucose metabolism, which results in closure of ATP-sensitive K^+ channels (K_{ATP} channels), membrane depolarization and opening of voltage-dependent Ca^{2+} channels. The resulting increase in $[Ca^{2+}]_i$ triggers exocytosis of insulin granules [16]. The increased ATP/ADP ratio also energizes the sarco/endoplasmic reticulum Ca^{2+}-ATPase (SERCA) to pump Ca^{2+} into the endoplasmic reticulum (ER), reflected as an immediate decrease in $[Ca^{2+}]_i$ preceding the depolarization-triggered Ca^{2+} entry when the cells are stimulated with glucose [17]. Filling of the ER Ca^{2+} stores prepares the β-cell to respond to neurotransmitters, including acetylcholine, which modulate secretion *via* G-protein-coupled receptors and phospholipase C-mediated generation of inositol 1,4,5-trisphosphate (IP_3) [18].

The aim of this study was to clarify how genetically encoded Ca^{2+} indicators and fluorescent dyes report $[Ca^{2+}]_i$ increases in β-cells triggered by depolarization with high $[K^+]$ and glucose. Pronounced differences were observed in sub-membrane Ca^{2+} signalling reported by the protein-based R-GECO1 and GCaMP5G sensors *versus* the synthetic dyes Fluo-4 and Fluo-5F. The differences highlight the occurrence of local, intracellular Ca^{2+} release events triggered by autocrine purinergic signalling in β-cells.

2. Materials and methods

2.1. Materials

Reagents of analytical grade and deionized water were used. Sigma Chemical (St Louis, MO, USA) was the source of diazoxide, EGTA, HEPES, cyclopiazonic acid, adenosine 5′-triphosphate magnesium salt and poly-L-lysine. The $P2Y_1$ receptor antagonist MRS2179 was purchased from Tocris Bioscience (Bristol, UK). The acetoxymethyl (AM) esters of the fluorescent Ca^{2+} dyes Fluo-5F and Fluo-4 were obtained from Life technologies. The genetically encoded Ca^{2+} indicators R-GECO1 [10] and GCaMP5G [19] were obtained from Addgene (plasmids #45494, a gift from Robert Campbell, and #31788, a gift from Loren Looger). β-cell-specific expression of R-GECO1 in islets was achieved by replacing the cytomegalovirus promoter with the rat insulin promoter 2 [20] to generate Ins-R-GECO1. Adenovirus production was performed at Vector Biolabs (Philadelphia, PA, USA). All cell culture reagents were from Life technologies.

2.2. MIN6 cell and islet culture and expression of genetically encoded indicators

Insulin-secreting MIN6 β-cells [21] (passages 18–32) were cultured in DMEM with 25 mM glucose and supplemented with 2 mM glutamine, 100 μg/ml streptomycin, 50 μM 2-mercaptoethanol, 15% FCS and 100 U/ml penicillin, and kept in 37 °C, 5% CO_2 humidified air atmosphere. For transfection, around 0.2 million cells were resuspended in Opti-MEM® medium containing Ca^{2+} sensor plasmid and Lipofectamine 2000 according to the manufacturer's protocol. The transfected cells were seeded onto the centre of a 25-mm poly-L-lysine-coated coverslips and cultured for 18–24 h to allow expression of the reporter protein.

Pancreatic islets were collagenase-isolated from 4 to 11 months old C57BL/6J mice (Taconic, Lille Skensved, Denmark). All procedures for animal handing were approved by the Uppsala animal ethics committee. After washing, the islets were cultured in RPMI 1640 medium (containing 100 U/ml penicillin, 100 μg/ml streptomycin, 5.5 mM glucose and 10% FCS) at 37 °C in an atmosphere of 5% CO_2 in humidified air. For Ca^{2+} measurements, the islets were infected with adenoviruses encoding R-GECO1 for 1.5–2 h and then further cultured overnight.

Human islets from four donors (2 males, 2 females, aged 19–67 years) were provided by the Nordic Network for Clinical Islet Transplantation in Uppsala. After delivery to the laboratory, the isolated islets were kept for 24 to 72 h in 37 °C, 5% CO_2 humidified air atmosphere in CMRL 1066 culture medium with 5.5 mM glucose, 2 mM glutamine, 100 U/ml penicillin, 100 μg/ml streptomycin and 10% FCS.

2.3. Recordings of $[Ca^{2+}]_i$

R-GECO1- and GCaMP5G-expressing cells were pre-incubated 30 min in experimental buffer containing 125 mM NaCl, 4.8 mM KCl, 1.3 mM $CaCl_2$, 1.2 mM $MgCl_2$, 3 mM glucose, and 25 mM HEPES (pH subsequently adjusted to 7.40 with NaOH). In experiments using the fluorescent Ca^{2+} dyes, the cells were incubated with 0.3–3 μM of Fluo-4 or Fluo-5F AM ester during 30 min at 37 °C in experimental buffer followed by washing in indicator-free buffer. The coverslips with cells were mounted in a 50-μl chamber, superfused at 0.3 ml/min with experimental buffer and placed on the microscope stage. The buffer and chamber were maintained at 37 °C. Fluorescence was recorded with total internal reflection fluorescence (TIRF) or widefield microscopy.

TIRF microscopy was used to record $[Ca^{2+}]_i$ in the sub-plasma membrane space. For MIN6 cells, the setup was based on an E600FN upright microscope (Nikon) with a 16×, NA 0.8 water immersion objective. The excitation laser beam was focused onto a modified quartz dove prism with 70° angle to achieve total internal reflection. For mouse islets, an objective-based system with a 60×, 1.45-NA oil immersion objective was used. Laser light was coupled to a TIRF illuminator attached to an inverted Nikon Eclipse Ti microscope. In both setups, R-GECO1 was excited at 561 nm and GCaMP5G/Fluo-5F/Fluo-4 at 491 nm, using diode-pumped solid-state lasers (Cobolt AB, Solna, Sweden). Fluorescence was detected at >593 nm (R-GECO1) and 530/35 nm (center wavelength/ half bandwidth) with a back-illuminated EMCCD camera (DU-897 Andor Technology, Tubney Woods, Abingdon, UK) controlled by MetaFluor software (Molecular Devices, Downingtown, PA, USA). If not otherwise stated, all filters were from Semrock, IDEX Health & Science, LLC, Rochester, NY, USA.

Widefield fluorescence imaging was performed with an Eclipse TE2000 microscope (Nikon) equipped with a 40×, 1.3-NA objective and an epifluorescence illuminator connected to an LED light source (Led-HUB, Omicron Laserage Laserprodukte GmbH, Rodgau, Germany). Diodes and bandpass filters were used to achieve excitation at 488/10 nm for Fluo-5F and Fluo-4, and 561/4 nm for R-GECO1. Emission was measured at 525/50 nm (Fluo-5F/Fluo-4) and 609/62 nm (R-GECO1) using a ZT 405–440/514/561 rpc-UF1 dichroic mirror (Chroma Technology Group) and an EMCCD camera (DU-897 Andor Technology) under MetaFluor control. In both the TIRF and widefield setups, images were acquired every 2–3 s.

2.4. Fluorescence recovery after photobleaching (FRAP)

To investigate the mobility of the Ca^{2+} indicators, FRAP experiments were performed in an objective-based TIRF system (Nikon 63×, NA 1.49) with an illuminator for targeted laser beam control (iLAS2, Gataca Systems, Massy, France). Coherent Obis solid-state lasers (491 and 561 nm) were used for excitation, a 491/561 dual-band dichroic (Chroma Technology) and 527/27 and 590 long-pass filters (Semrock) were used for emission detected by an iXon DU-897 EMCCD camera (Andor Technology). Images were acquired at 2 Hz. A 3.5-μm diameter area within the cells was exposed to a 100 ms pulse of 405 nm laser light (Coherent Obis) to bleach the fluorophores. To calculate the mobile fraction of each Ca^{2+} indicator, the following equation was used [22]:

$$\text{Mobile fraction} = 100 * \frac{(Fpc - Fbg)}{(F\infty c - Fbg)} * \frac{((F\infty - Fbg) - (F0 - Fbg))}{((Fp - Fbg) - (F0 - Fbg))}$$

Fpc denotes the whole-cell pre-bleach intensity; Fp is the bleach region of interest (ROI) pre-bleach intensity; F∞c is the asymptote of fluorescence recovery of the whole cell; Fbg is the mean background intensity; F∞ is the asymptote of the bleach ROI; and F0 is the bleach ROI post-bleach intensity.

2.5. Plasma membrane permeabilization

To determine the Ca^{2+} sensitivity of the Ca^{2+} indicators, the cells were permeabilized with α-toxin from *Staphylococcus aureus* (PhPlate Stockholm, Stockholm, Sweden) in an intracellular-like medium containing 6 mM NaCl, 140 mM KCl, 1 mM Mg-ATP, 2 mM EGTA, 2 mM HEDTA, 2 mM NTA and 10 mM HEPES with pH adjusted to 7.0. The superfusion was stopped and α-toxin (5 μl, 0.46 mg/ml) was added directly to the chamber. After 15–20 min the cells were washed. The concentration of free Ca^{2+} was subsequently increased in steps from 0.1 μM to 300 μM. The amount of $CaCl_2$ to be added was determined with the online Maxchelator program (https://somapp.ucdmc.ucdavis.edu/pharmacology/bers/maxchelator/webmaxc/webmaxcS.htm). The calculated free Mg^{2+} concentration varied from 34 μM in the absence of Ca^{2+} to 208 μM in the buffer with 300 μM Ca^{2+}.

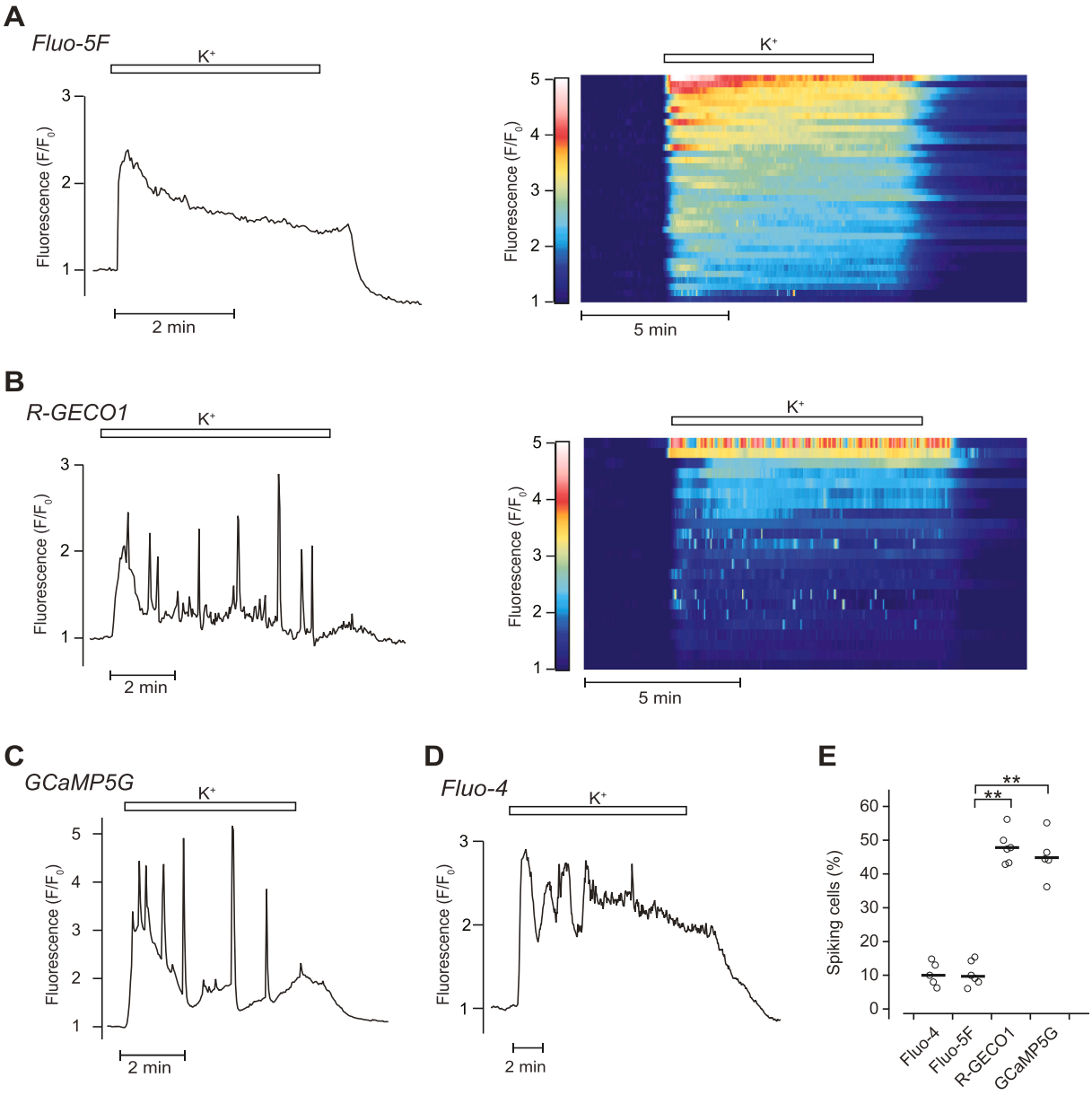

Fig. 1. Genetically encoded Ca^{2+} indicators unmask depolarization-triggered $[Ca^{2+}]_i$ spikes in β-cells.
A, TIRF recordings of submembrane $[Ca^{2+}]_i$ from MIN6 cells loaded with Fluo-5F and depolarized with 30 mM K^+. Single-cell example trace and heat map representing data from one experiment. The fluorescence signals from individual cells were normalized to the baseline (F/F_0) and sorted by the amplitude of the response to depolarization. Each line shows the response from one cell. Representative of in total 171 cells from 6 experiments.
B, Similar recordings from cells expressing R-GECO1. $n = 184$ cells from 6 experiments.
C, Representative $[Ca^{2+}]_i$ recording from a single cell expressing GCaMP5G. $n = 153$ cells from 5 experiments.
D, Representative $[Ca^{2+}]_i$ recording from a single cell loaded with Fluo-4. $n = 121$ cells from 5 experiments.
E, Medians for the percentage of cells showing $[Ca^{2+}]_i$ spikes with different Ca^{2+} indicators. Each data point represents the percentage in 1 experiment. $^{**}P < 0.01$ for difference from Fluo-5F (Mann-Whitney test).

2.6. Image analysis and statistics

All experiments were performed with cells from at least 3 different passages or islet isolations. Background-subtracted images from the TIRF and widefield microscopes were analysed off-line using MetaFluor. Igor Pro software (Wavemetrics, Lake Oswego, OR) was used for data analysis and together with Illustrator (Adobe Systems, San Jose, CA) for preparation of illustrations. Fluorescence intensities from single cells (F) were normalized to the initial prestimulatory intensity (F_0) and expressed as (F/F_0). $[Ca^{2+}]_i$ spikes were defined as deviations of >20% from the prevailing fluorescence level.

3. Results

3.1. Genetically encoded Ca^{2+} indicators unmask depolarization-triggered $[Ca^{2+}]_i$ spikes in β-cells

$[Ca^{2+}]_i$ was recorded with TIRF microscopy from the sub-plasma membrane space of MIN6 cells expressing R-GECO1 or loaded with Fluo-5F. Irrespective of Ca^{2+} indicator, $[Ca^{2+}]_i$ was stable in cells exposed to basal medium containing 3 mM glucose. Depolarization of the plasma membrane by elevation of $[K^+]$ to 30 mM triggered a prompt increase of $[Ca^{2+}]_i$. In the vast majority of Fluo-5F-loaded cells (≈90%), the initial increase was followed by a stable $[Ca^{2+}]_i$ elevation (Fig. 1A). The remaining cells showed occasional $[Ca^{2+}]_i$ spikes (duration≈10 s) from an elevated level. In contrast, such spikes were observed in about 50% of the R-GECO1-expressing cells (Fig. 1B, E). $[Ca^{2+}]_i$ spikes were frequently observed also with the protein-based indicator GCaMP5G (Fig. 1C, E), whereas the dye Fluo-4 mostly reported stable elevations (Fig. 1D, E).

3.2. Depolarization-triggered $[Ca^{2+}]_i$ spikes reflect Ca^{2+} release from the ER

The $[Ca^{2+}]_i$ spikes may reflect either Ca^{2+} entry through channels in the plasma membrane or release of the ion from the ER. To clarify the potential ER involvement, R-GECO1-expressing cells were exposed to 20 mM glucose and the K_{ATP} channel opener diazoxide (250 μM) to stimulate filling of the ER Ca^{2+} stores while hyperpolarizing the cells to maintain low, resting $[Ca^{2+}]_i$ [23]. Depolarization with high $[K^+]$ subsequently triggered spiking, which was selectively interrupted by ER Ca^{2+} depletion with the SERCA inhibitor cyclopiazonic acid (CPA, 100 μM) while the baseline elevation of $[Ca^{2+}]_i$ was maintained (Fig. 2A,D). Consistent with ER Ca^{2+} depletion, the muscarinic agonist carbachol (100 μM) showed little increase of $[Ca^{2+}]_i$ in the presence of CPA but washout of CPA both restored $[Ca^{2+}]_i$ spiking and a prominent response to carbachol (Fig. 2A).

3.3. $[Ca^{2+}]_i$ spiking involves activation of purinergic $P2Y_1$ receptors

Stimulated β-cells release ATP and ADP [24] resulting in autocrine activation of purinergic $P2Y_1$ receptors [25,26]. To clarify if the depolarization-triggered $[Ca^{2+}]_i$ spikes reflects such feedback with resulting activation of phospholipase C and IP_3-mediated mobilization of ER Ca^{2+}, depolarized cells were exposed to the $P2Y_1$ receptor antagonist MRS2179 (10 μM). This drug reversibly abolished depolarization-triggered $[Ca^{2+}]_i$ spiking (Fig. 2B, D). Similarly, introduction of the antagonist before depolarization prevented spiking until the drug was removed (Fig. 2C, D).

3.4. Glucose and K^+ depolarization trigger $[Ca^{2+}]_i$ spiking in primary mouse and human β-cells

To investigate whether the spikes reflect a physiologically relevant

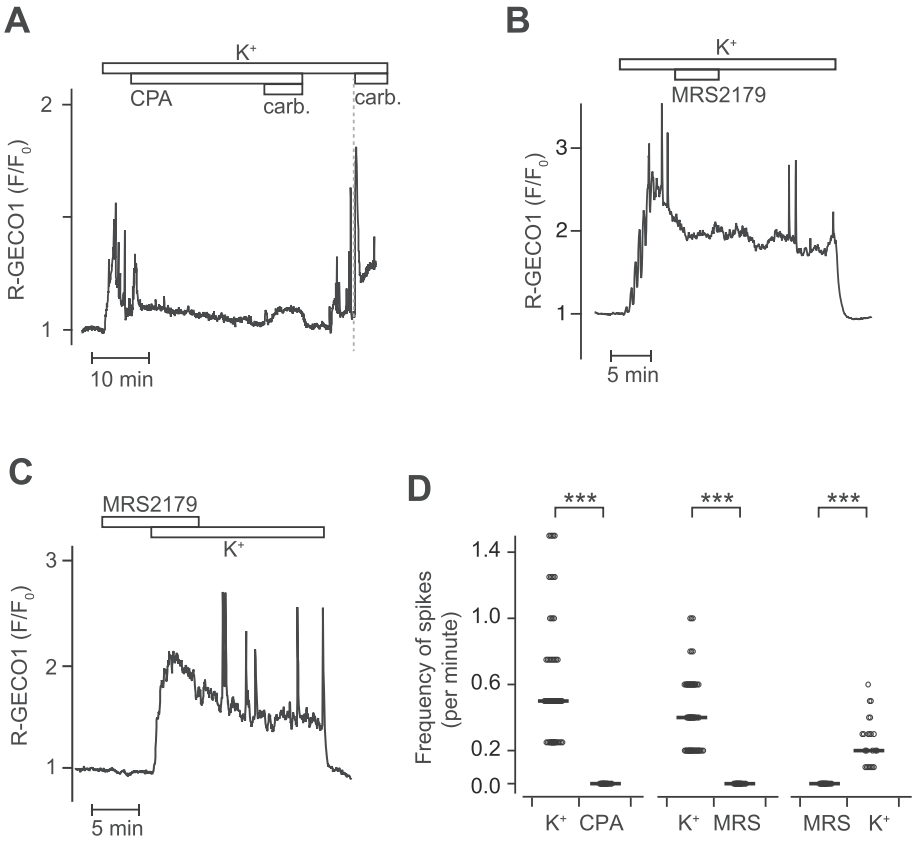

Fig. 2. The depolarization-triggered $[Ca^{2+}]_i$ spikes reflect Ca^{2+} release from the ER triggered by purinergic $P2Y_1$ receptor activation.
A, TIRF recording of $[Ca^{2+}]_i$ from a single R-GECO1-expressing MIN6 cell exposed to 20 mM glucose, 250 μM diazoxide, 30 mM K^+, 100 μM CPA and 100 μM carbachol (carb) as indicated. $n = 73$ cells from 3 experiments.
B, **C**, Similar recordings with 10 μM of the $P2Y_1$ receptor antagonist MRS2179. $n = 78$ spiking cells out of 136 from 3 experiments (B) and 23 spiking cells out of 56 from 2 experiments (C).
D, Medians for the frequency of $[Ca^{2+}]_i$ spikes in experiments as in A-C. $^{***}P < 0.001$, Wilcoxon test.

phenomenon, we used intact pancreatic islets and stimulated them with the natural insulin secretagogue glucose. Both mouse and human islet cells expressing R-GECO1 responded to 20 mM glucose with MRS2179-sensitive $[Ca^{2+}]_i$ spikes (Fig. 3A-C). The spiking ceased when the membrane was hyperpolarized with the K_{ATP}-channel opener diazoxide but reappeared upon depolarization with high $[K^+]$. Since islets contain excitable cells other than β-cells, including α- and δ-cells, it was confirmed that similar glucose- and K^+-triggered $[Ca^{2+}]_i$ spiking was observed also when the indicator was specifically expressed in β-cells using the insulin promoter (Fig. 3D, E).

3.5. Indicator-dependent differences in $[Ca^{2+}]_i$ spike detection are unrelated to Ca^{2+} buffering

Since Ca^{2+} buffering has been found to prevent the occurrence of fast $[Ca^{2+}]_i$ changes [27], recordings were performed after a tenfold reduction in dye loading concentration. With both Fluo-5F and Fluo-4, there was only a tendency to increased spiking and higher spike amplitudes but not in frequency after loading with 0.3 compared to 3 μM AM-dye (Suppl. Fig. 1). Moreover, when R-GECO1-expressing cells were loaded with Fluo-5F (3 μM AM-dye), the dye often showed stable $[Ca^{2+}]_i$ elevation, while the protein indicator reported spikes from the same cell (Fig. 4A, B).

3.6. R-GECO1, Fluo-5F and Fluo-4 show similar Ca^{2+} sensitivities in situ

Since differences in Ca^{2+} affinity potentially may explain the different $[Ca^{2+}]_i$ responses, the Ca^{2+} sensitivities of R-GECO1, Fluo-5F and Fluo-4 were investigated in cells permeabilized with α-toxin. R-GECO1 fluorescence showed little change upon permeabilization, since

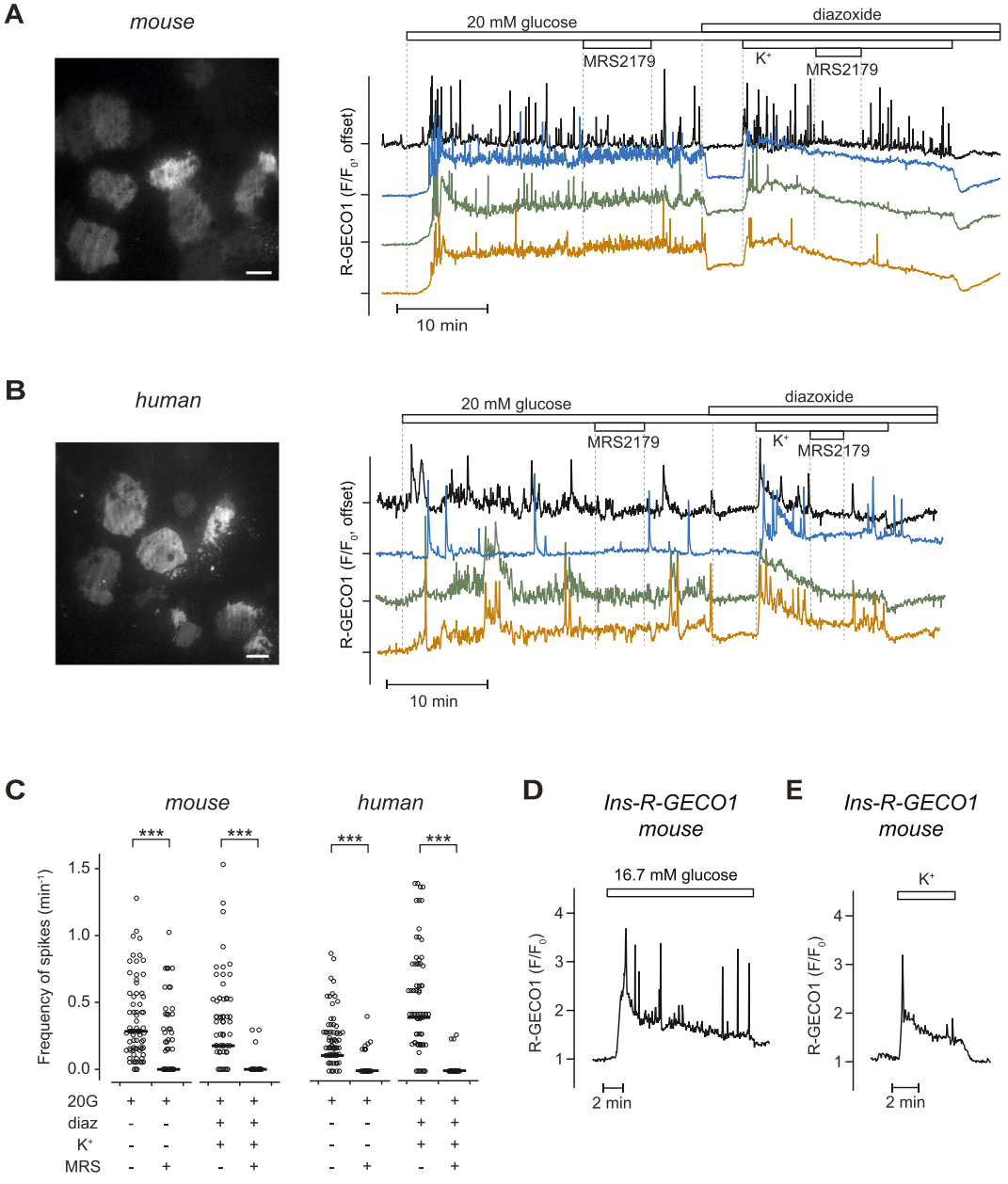

Fig. 3. Glucose and K^+ depolarization trigger $[Ca^{2+}]_i$ spiking in primary mouse and human β-cells.
A, B, TIRF images and corresponding recordings of $[Ca^{2+}]_i$ from R-GECO1-expressing cells within an intact mouse (A) and a human (B) islet exposed to 20 mM glucose, 250 μM diazoxide, 30 mM K^+ and 10 μM MRS2179 as indicated. Representative of 102 (A) and 72 (B) cells from 4 experiments with each species.
C, Medians for the frequency of $[Ca^{2+}]_i$ spikes in experiments as in A and B. ***$P < 0.001$ for the effects of MRS2179 (Wilcoxon test).
D, E, TIRF recordings of $[Ca^{2+}]_i$ from mouse β-cells identified by expression of Ins-R-GECO1. Representative of 40 cells from 3 recordings.

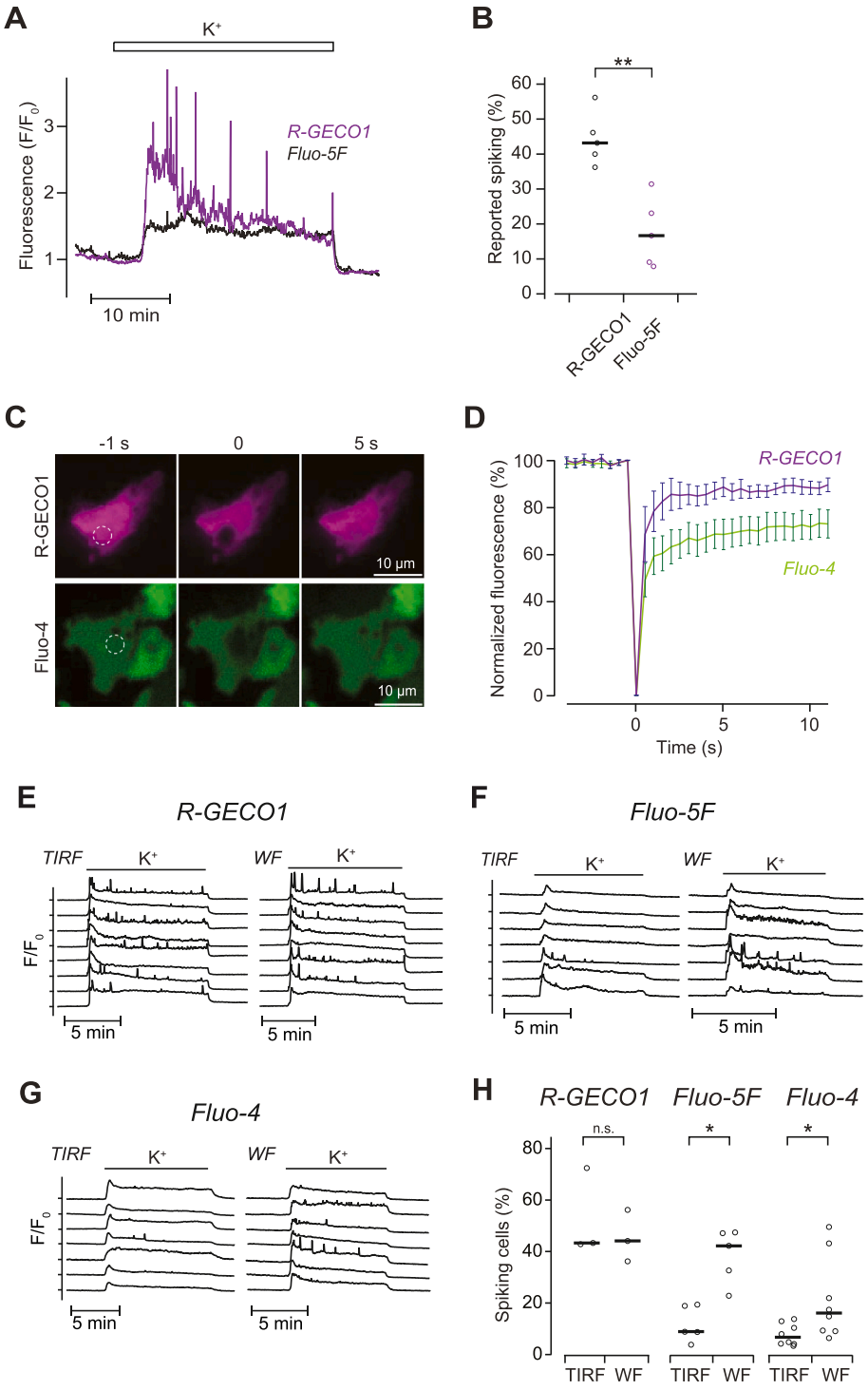

Fig. 4. Indicator buffering and mobility and the influence of imaging mode for detecting $[Ca^{2+}]_i$ spikes.
A, $[Ca^{2+}]_i$ recorded simultaneously with R-GECO1 and Fluo-5F from a single MIN6 cell depolarized with 30 mM K^+. Representative of 272 cells from 5 experiments.
B, Medians for the percentage of cells showing spikes reported with R-GECO1 and Fluo-5F in MIN6 cells containing both indicators like in A. **P < 0.01 for difference (Wilcoxon test).
C, TIRF images of R-GECO1 or Fluo-4 expressing cells before, during and 5 s after a bleaching laser pulse in FRAP experiments. The dashed circle indicates the bleach region.
D. Means±s.e.m. for the normalized fluorescence intensity changes in FRAP experiments. Time = 0 indicates the end of a 100 ms bleach laser exposure.
***E*-G,** $[Ca^{2+}]_i$ responses to K^+ depolarization recorded in TIRF or widefield (WF) imaging modes with R-GECO1 (E), Fluo-5F (F) and Fluo-4 (G). Traces representative of 101 and 300 cells from 3 experiments experiments with R-GECO1 in TIRF and WF, respectively (E); 289 and 315 cells from 5 experiments with Fluo-5F in TIRF and WF, respectively (F); and 547 and 886 cells from 8 experiments with Fluo-4 in TIRF and WF (G).
H, Medians for the percentage of spiking cells detected with different Ca^{2+} indicators in TIRF and widefield (WF) imaging modes. *$P < 0.05$, Mann-Whitney test.

the indicator cannot escape through the α-toxin pores. In contrast, Fluo-4 and Fluo-5F fluorescence decreased as the dyes leaked from the cytoplasm but 15–30% of the signal remained after permeabilization, allowing recordings from retained dye. Permeabilized cells were superfused with intracellular-like buffer with increasing Ca^{2+} concentrations in the 0–300 µM range. All indicators responded to Ca^{2+} with a rapid increase of fluorescence to a new steady-state (Suppl. Fig. 2). Half-maximal fluorescence increases were observed at 3.0 ± 0.3, 2.4 ± 0.4 and 1.7 ± 0.1 µM Ca^{2+} for R-GECO1, Fluo-4 and Fluo-5F, respectively (Suppl. Fig. 2D), indicating rather similar and low Ca^{2+} sensitivities *in situ*.

3.7. FRAP analysis shows no major differences in mobility between R-GECO1 and Fluo-4

To investigate whether differences in spike detection may be explained by differences in indicator mobility, a small region was photobleached and the rate and fraction of fluorescence recovery determined. There was no measurable difference in the rate of recovery at a time-scale relevant for the spikes. Whereas the mobile fraction of R-GECO1 was 89 ± 2% ($n = 7$), a lower fraction was observed for Fluo-4 (72 ± 5%; $n = 8$; $P < 0.02$; Fig. 4C, D), mirroring the proportion of diffusible dye that was released after cell permeabilization.

3.8. Wide-field imaging facilitates spike detection with the dyes

Given that $[Ca^{2+}]_i$ spikes reflect intracellular Ca^{2+} release, it was tested if widefield imaging of the entire cytoplasm facilitated spike detection compared to TIRF imaging of a restricted submembrane compartment. Whereas similar fractions of R-GECO1-expressing MIN6 cells showed $[Ca^{2+}]_i$ spikes in widefield and TIRF imaging modes, a significantly higher proportion of cells loaded with Fluo-5F or Fluo-4 showed spiking in widefield compared to TIRF mode (Fig. 4E-H). This finding may reflect the known difference in Ca^{2+} dissociation kinetics between dyes and protein indicators (see below).

4. Discussion

The present study revealed differences in how genetically encoded indicators and fluorescent dyes report $[Ca^{2+}]_i$ kinetics in response to plasma membrane depolarization in β-cells. Cells expressing R-GECO1 and GCaMP5G often showed pronounced spikes with a duration of about 10 s under conditions when the synthetic dye indicators reported stable $[Ca^{2+}]_i$ elevation. Submembrane $[Ca^{2+}]_i$ spiking has been reported to occur in β-cells as a consequence of voltage-dependent Ca^{2+} channel activity [28] or release from acidic Ca^{2+} stores [29]. However, the pattern now observed was considerably slower and turned out to reflect release of Ca^{2+} from the ER, since the spikes were abolished by SERCA inhibition. Depolarization-evoked increases of $[Ca^{2+}]_i$ have been found to activate phospholipase C in β-cells [30,31] as well as inositol 1,4,5-trisphosphate receptor-mediated calcium-induced calcium release [32]. Also ryanodine receptors have been suggested to mediate calcium-induced calcium release in β-cells [33], but the involvement of these receptors has been disputed [32]. Since it is difficult to dissociate $[Ca^{2+}]_i$ elevation from exocytosis, some of the effect may reflect activation of phospholipase C by factors secreted from the β-cells rather than by Ca^{2+} itself. Apart from being present in the β-cell cytoplasm, ATP and ADP are concentrated in the secretory granules [24] and are co-released with insulin during exocytosis [34]. The released adenine nucleotides activate purinergic $P2Y_1$ receptors on the β-cell plasma membrane in an auto- and paracrine fashion [25,26]. This signalling results in parallel spikes of the membrane lipid diacylglycerol [25] and seem to exert feedback control of secretion, potentially *via* the protein *E*-Syt1 [35]. The present observation that a $P2Y_1$ receptor antagonist abolished the $[Ca^{2+}]_i$ spikes strongly indicates that the spikes reflect the same purinergic feedback loop.

It is not immediately evident why the protein-based Ca^{2+} indicators detect $[Ca^{2+}]_i$ release events in the submembrane space. Differences in Ca^{2+} binding affinity did not seem to explain the different kinetics. The Ca^{2+} concentration dependencies now determined *in situ* in permeabilized cells differed from previously reported *in vitro* properties. For example, the reported K_d value of R-GECO1 is 480 nM [10], which is close to that reported for Fluo-4, but whereas the present permeabilization experiments now indicated a half-maximal fluorescence change at approximately 3 μM. Also Fluo-4 showed lower affinity than previously reported [2], but the population of dye molecules bound to intracellular structures or trapped inside organelles, and therefore remaining after permeabilization, likely has different properties than freely diffusible indicator. However, the same approach yielded values for Fluo-5F that compares well with the previously reported K_d [3]. Irrespective of whether *in vitro* or *in situ* determined values are considered, different $[Ca^{2+}]_i$ responses were observed with indicators of comparable Ca^{2+} sensitivities.

The different indicators could potentially exert varying degrees of Ca^{2+} buffering. Such variations may not only reflect the indicators' Ca^{2+} binding affinities, but also their intracellular concentrations. Dyes have been reported to reach higher cytoplasmic concentrations than protein-based indicators [6] but the precise concentrations in the present β-cell experiments are not known. It was previously reported that reduced dye indicator concentrations favour detection of Ca^{2+} spikes in β-cells [27] but under the conditions tested here, this effect was rather marginal. If the dyes by buffering or other means inhibit exocytosis, fewer spikes would be expected in dye-loaded cells. However, the observation that the different responses of R-GECO1 and Fluo-5F remain when present in the same cell provides arguments against both buffering and any other dye-mediated disruptive effect on cell function [6,7].

The study set out to investigate voltage-dependent Ca^{2+} influx and TIRF microscopy was therefore applied to selectively record $[Ca^{2+}]_i$ from the submembrane compartment. In line with the $[Ca^{2+}]_i$ spikes originating from the ER, we found that widefield imaging throughout the cytoplasm facilitated spike detection with the dye indicators. It should not be surprising if intracellular Ca^{2+} release events evade detection with submembrane recordings, since most of the release events would occur outside the excited volume in the deeper cytoplasm and the restricted diffusion of Ca^{2+} [36] would make the relative contribution to the fluorescence signal small in relation to that from voltage-dependent Ca^{2+} entry that dominates in the periphery. The explanation for the different detection of submembrane Ca^{2+} signals by protein and dye indicators remains unclear. A higher cooperativity of Ca^{2+} binding for the protein-based indicators [10] may enhance the appearance of the spikes. We speculate that the different Ca^{2+} dissociation kinetics of the indicator classes also contribute. R-GECO1 has nearly three orders of magnitude slower Ca^{2+} dissociation rate compared to indicator dyes [10,37]. Reported values for diffusion coefficients are not grossly different [37–39], a conclusion supported by the present FRAP experiments. The linear average diffusion distance, s, can be described as $s = (4Dt/\pi)^{0.5}$, where D is the diffusion coefficient and t is the time of diffusion. A three orders of magnitude difference in t (derived from k_{off}), will result in a ≈ 30-fold difference in diffusion distance. With a k_{off} of 0.752 s^{-1} [10], R-GECO1 would be able to diffuse a distance corresponding to the radius of a β-cell (≈6 μm assuming a D of 20 $\mu m^2/s$ as for GFP [38]) before releasing Ca^{2+}, whereas the dyes would only reach ≈0.4 μm (assuming D = 75 $\mu m^2/s$ as reported for Fluo-5F [37]). Thus, irrespective of where a Ca^{2+} release event takes place, the Ca^{2+}-bound protein indicator will more likely reach the submembrane compartment imaged by the evanescent field than the dye indicator. Accordingly, widefield imaging only increased spike detection with the dye indicators and not the protein indicators.

The fact that dye indicators did not readily report $[Ca^{2+}]_i$ spiking in the sub-membrane compartment can be taken as evidence that granular release of adenine nucleotides usually does not trigger global autocrine purinergic signalling. Instead, the data indicate that $P2Y_1$ receptors are activated only close to the release site, triggering spatially restricted IP_3 production and local ER Ca^{2+} release. This conclusion is in agreement with generation of diacylglycerol microdomains in β-cells following similar autocrine $P2Y_1$ receptor activation [25]. That the slow kinetics of protein-based Ca^{2+} indicators make them less suitable than dyes to detect IP_3-induced local, subcellular Ca^{2+} signals have been noted also in neuroblastoma cells [11]. Protein Ca^{2+} indicators modified for faster dissociation kinetics should be promising alternatives to dyes for more faithful monitoring of local Ca^{2+} release events [40].

In conclusion, the different properties of synthetic Ca^{2+} dyes and genetically encoded indicators may substantially influence how $[Ca^{2+}]_i$ signals appear in TIRF and widefield imaging modes. Sub-membrane Ca^{2+} signals may be contaminated by intracellular release events when using protein indicators with slow dissociation kinetics. Direct comparison of different types of indicators may help to unmask important features of cell physiology. In β-cells, the strong link between Ca^{2+} influx and intracellular release has previously been attributed to CICR [32,33] and direct activation of PLC [30,31]. The present study reinforces an important role of purinergic autocrine feedback signalling in this process, a phenomenon that has been largely overlooked with Ca^{2+} dyes.

CRediT authorship contribution statement

Mingyu Yang: Investigation, Formal analysis, Writing – original

draft. **Oleg Dyachok:** Conceptualization, Formal analysis, Writing – review & editing. **Yunjian Xu:** Resources. **Erik Gylfe:** Conceptualization, Writing – review & editing. **Olof Idevall-Hagren:** Conceptualization, Writing – review & editing, Funding acquisition. **Anders Tengholm:** Conceptualization, Supervision, Writing – review & editing, Funding acquisition.

Declaration of Competing Interest

The authors have no competing interests to declare.

Data availability

Data will be made available on request.

Acknowledgements

This work was supported by grants from the Swedish Research Council (2019-01456; 2021-02081), Swedish Diabetes Foundation, Diabetes Wellness Foundation, Family Ernfors Foundation, Novo Nordisk Foundation (NNF19OC005275, NNF20OC0064000), The Leona M and Harry B Helmsley Charitable Trust, the Swedish Child Diabetes Foundation and the Swedish national strategic grant initiative EXODIAB (Excellence of diabetes research in Sweden). Human islets were generously provided by the Nordic Network for Clinical Islet Transplantation supported by EXODIAB.

Appendix A. Supplementary data

Supplementary data to this article can be found online at https://doi.org/10.1016/j.cellsig.2023.110805.

References

[1] G. Grynkiewicz, M. Poenie, R.Y. Tsien, A new generation of Ca^{2+} indicators with greatly improved fluorescence properties, J. Biol. Chem. 260 (1985) 3440–3450.
[2] K.R. Gee, K.A. Brown, W.N. Chen, J. Bishop-Stewart, D. Gray, I. Johnson, Chemical and physiological characterization of fluo-4 Ca^{2+}-indicator dyes, Cell Calcium 27 (2000) 97–106.
[3] H.R. Matthews, G.L. Fain, A light-dependent increase in free Ca^{2+} concentration in the salamander rod outer segment, J. Physiol. 532 (2001) 305–321.
[4] P. Lipp, E. Niggli, Ratiometric confocal Ca^{2+}-measurements with visible wavelength indicators in isolated cardiac myocytes, Cell Calcium 14 (1993) 359–372.
[5] C. Tischbirek, A. Birkner, H. Jia, B. Sakmann, A. Konnerth, Deep two-photon brain imaging with a red-shifted fluorometric Ca^{2+} indicator, Proc. Natl. Acad. Sci. U. S. A. 112 (2015) 11377–11382.
[6] P. Robinson, A.J. Sparrow, Y. Psaras, V. Steeples, J. Simon, C.N. Broyles, Y. F. Chang, F.A. Brook, Y.J. Wang, A. Blease, X. Zhang, Y.A. Abassi, M.A. Geeves, C. N. Toepfer, H. Watkins, C. Redwood, M.J. Daniels, Comparing the effects of chemical Ca^{2+} dyes and R-GECO on contractility and Ca^{2+} transients in adult and human iPSC cardiomyocytes, J. Mol. Cell. Cardiol. 180 (2023) 44–57.
[7] N.A. Smith, B.T. Kress, Y. Lu, D. Chandler-Militello, A. Benraiss, M. Nedergaard, Fluorescent Ca^{2+} indicators directly inhibit the Na,K-ATPase and disrupt cellular functions, Sci. Signal. 11 (2018).
[8] A. Miyawaki, J. Llopis, R. Heim, J.M. McCaffery, J.A. Adams, M. Ikura, R.Y. Tsien, Fluorescent indicators for Ca^{2+} based on green fluorescent proteins and calmodulin, Nature 388 (1997) 882–887.
[9] J. Nakai, M. Ohkura, K. Imoto, A high signal-to-noise Ca^{2+} probe composed of a single green fluorescent protein, Nat. Biotechnol. 19 (2001) 137–141.
[10] Y. Zhao, S. Araki, J. Wu, T. Teramoto, Y.F. Chang, M. Nakano, A.S. Abdelfattah, M. Fujiwara, T. Ishihara, T. Nagai, R.E. Campbell, An expanded palette of genetically encoded Ca^{2+} indicators, Science 333 (2011) 1888–1891.
[11] J.T. Lock, I. Parker, I.F. Smith, A comparison of fluorescent Ca^{2+} indicators for imaging local Ca^{2+} signals in cultured cells, Cell Calcium 58 (2015) 638–648.
[12] E. Grapengiesser, E. Gylfe, B. Hellman, Glucose-induced oscillations of cytoplasmic Ca^{2+} in the pancreatic β-cell, Biochem. Biophys. Res. Commun. 151 (1988) 1299–1304.
[13] P. Gilon, J.C. Henquin, Influence of membrane potential changes on cytoplasmic Ca^{2+} concentration in an electrically excitable cell, the insulin-secreting pancreatic B-cell, J. Biol. Chem. 267 (1992) 20713–20720.
[14] P. Rorsman, H. Abrahamsson, E. Gylfe, B. Hellman, Dual effects of glucose on the cytosolic Ca^{2+} activity of mouse pancreatic beta-cells, FEBS Lett. 170 (1984) 196–200.
[15] O. Idevall-Hagren, A. Tengholm, Metabolic regulation of calcium signaling in beta cells, Semin. Cell Dev. Biol. 103 (2020) 20–30.
[16] P. Rorsman, F.M. Ashcroft, Pancreatic β-cell electrical activity and insulin secretion: of mice and men, Physiol. Rev. 98 (2018) 117–214.
[17] R.H. Chow, P.E. Lund, S. Löser, U. Panten, E. Gylfe, Coincidence of early glucose-induced depolarization with lowering of cytoplasmic Ca^{2+} in mouse pancreatic β-cells, J. Physiol. 485 (1995) 607–617.
[18] P. Gilon, J.C. Henquin, Mechanisms and physiological significance of the cholinergic control of pancreatic β-cell function, Endocr. Rev. 22 (2001) 565–604.
[19] J. Akerboom, T.W. Chen, T.J. Wardill, L. Tian, J.S. Marvin, S. Mutlu, N. C. Calderon, F. Esposti, B.G. Borghuis, X.R. Sun, A. Gordus, M.B. Orger, R. Portugues, F. Engert, J.J. Macklin, A. Filosa, A. Aggarwal, R.A. Kerr, R. Takagi, S. Kracun, E. Shigetomi, B.S. Khakh, H. Baier, L. Lagnado, S.S. Wang, C. I. Bargmann, B.E. Kimmel, V. Jayaraman, K. Svoboda, D.S. Kim, E.R. Schreiter, L. L. Looger, Optimization of a GCaMP calcium indicator for neural activity imaging, J. Neurosci. 32 (2012) 13819–13840.
[20] H. Shuai, Y. Xu, Q. Yu, E. Gylfe, A. Tengholm, Fluorescent protein vectors for pancreatic islet cell identification in live-cell imaging, Pflügers Arch. 468 (2016) 1765–1777.
[21] J. Miyazaki, K. Araki, E. Yamato, H. Ikegami, T. Asano, Y. Shibasaki, Y. Oka, K. Yamamura, Establishment of a pancreatic β cell line that retains glucose-inducible insulin secretion: special reference to expression of glucose transporter isoforms, Endocrinology 127 (1990) 126–132.
[22] E.L. Snapp, N. Altan, J. Lippincott-Schwartz, Measuring protein mobility by photobleaching GFP chimeras in living cells, Curr Protoc Cell Biol (2003), https://doi.org/10.1002/0471143030.cb2101s19.
[23] E. Gylfe, Carbachol induces sustained glucose-dependent oscillations of cytoplasmic Ca^{2+} in hyperpolarized pancreatic β cells, Pflügers Archiv, Eur. J. Phys. 419 (1991) 639–643.
[24] J.W. Leitner, K.E. Sussman, A.E. Vatter, F.H. Schneider, Adenine nucleotides in the secretory granule fraction of rat islets, Endocrinology 96 (1975) 662–677.
[25] A. Wuttke, O. Idevall-Hagren, A. Tengholm, $P2Y_1$ receptor-dependent diacylglycerol signaling microdomains in β cells promote insulin secretion, FASEB J. 27 (2013) 1610–1620.
[26] S. Khan, R. Yan-Do, E. Duong, X. Wu, A. Bautista, S. Cheley, P.E. MacDonald, M. Braun, Autocrine activation of P2Y1 receptors couples Ca^{2+} influx to Ca^{2+} release in human pancreatic beta cells, Diabetologia 57 (2014) 2535–2545.
[27] O. Dyachok, G. Tufveson, E. Gylfe, Ca^{2+}-induced Ca^{2+} release by activation of inositol 1,4,5-trisphosphate receptors in primary pancreatic β-cells, Cell Calcium 36 (2004) 1–9.
[28] G. Langlhofer, A. Kogel, M. Schaefer, Glucose-induced $[Ca^{2+}]_i$ oscillations in beta cells are composed of trains of spikes within a subplasmalemmal microdomain, Cell Calcium 99 (2021), 102469.
[29] P.M. Heister, T. Powell, A. Galione, Glucose and NAADP trigger elementary intracellular β-cell Ca^{2+} signals, Sci. Rep. 11 (2021) 10714.
[30] T.J. Biden, B. Peter-Riesch, W. Schlegel, C.B. Wollheim, Ca^{2+}-mediated generation of inositol 1,4,5-trisphosphate and inositol 1,3,4,5-tetrakisphosphate in pancreatic islets. Studies with K^+, glucose, and carbamylcholine, J. Biol. Chem. 262 (1987) 3567–3571.
[31] S. Thore, O. Dyachok, A. Tengholm, Oscillations of phospholipase C activity triggered by depolarization and Ca^{2+} influx in insulin-secreting cells, J. Biol. Chem. 279 (2004) 19396–19400.
[32] O. Dyachok, E. Gylfe, Ca^{2+}-induced Ca^{2+} release via inositol 1,4,5-trisphosphate receptors is amplified by protein kinase a and triggers exocytosis in pancreatic β-cells, J. Biol. Chem. 279 (2004) 45455–45461.
[33] R. Lemmens, O. Larsson, P.O. Berggren, M.S. Islam, Ca^{2+}-induced Ca^{2+} release from the endoplasmic reticulum amplifies the Ca^{2+} signal mediated by activation of voltage-gated L-type Ca^{2+} channels in pancreatic β-cells, J. Biol. Chem. 276 (2001) 9971–9977.
[34] S. Obermüller, A. Lindqvist, J. Karanauskaite, J. Galvanovskis, P. Rorsman, S. Barg, Selective nucleotide-release from dense-core granules in insulin-secreting cells, J. Cell Sci. 118 (2005) 4271–4282.
[35] B. Xie, P.M. Nguyen, O. Idevall-Hagren, Feedback regulation of insulin secretion by extended synaptotagmin-1, FASEB J. 33 (2019) 4716–4728.
[36] N.L. Allbritton, T. Meyer, L. Stryer, Range of messenger action of calcium ion and inositol 1,4,5-trisphosphate, Science 258 (1992) 1812–1815.
[37] E. Hamid, E. Church, S. Alford, Quantitation and simulation of single action potential-Evoked Ca^{2+} signals in CA1 pyramidal neuron presynaptic terminals, eNeuro 6 (2019).
[38] E.O. Potma, W.P. de Boeij, L. Bosgraaf, J. Roelofs, P.J. van Haastert, D.A. Wiersma, Reduced protein diffusion rate by cytoskeleton in vegetative and polarized dictyostelium cells, Biophys. J. 81 (2001) 2010–2019.
[39] I. Delvendahl, L. Jablonski, C. Baade, V. Matveev, E. Neher, S. Hallermann, Reduced endogenous Ca^{2+} buffering speeds active zone Ca^{2+} signaling, Proc. Natl. Acad. Sci. U. S. A. 112 (2015) E3075–E3084.
[40] S. Kerruth, C. Coates, C.D. Durst, T.G. Oertner, K. Torok, The kinetic mechanisms of fast-decay red-fluorescent genetically encoded calcium indicators, J. Biol. Chem. 294 (2019) 3934–3946.